Biology of Reproduction, 2021, 105(1), 278–289
https://doi.org/10.1093/biolre/ioab069
Research Article
Advance Access Publication Date: 14 April 2021

Research Article

Obesity alters the ovarian proteomic response to zearalenone exposure†

M. Estefanía González-Alvarez, Bailey C. McGuire and Aileen F. Keating*

Department of Animal Science and Interdepartmental Toxicology Graduate Program, Iowa State University, Ames IA, USA

***Correspondence:** Department of Animal Science and Interdepartmental Toxicology Graduate Program, Iowa State University, 2356H Kildee Hall, 806 Stange Rd, Ames IA 50011, USA. Tel: 515-294-3849; E-mail: akeating@iastate.edu

†Grant Support: This study was funded by the Iowa State University Martin Fund from the Nutritional Science Council and the Bailey Career Development Award to AFK.

Received 20 November 2020; Revised 10 March 2021; Accepted 7 April 2021

Abstract

Zearalenone (ZEN), a nonsteroidal estrogenic mycotoxin, is detrimental to female reproduction. Altered chemical biotransformation, depleted primordial follicles and a blunted genotoxicant response have been discovered in obese female ovaries, thus, this study investigated the hypothesis that obesity would enhance ovarian sensitivity to ZEN exposure. Seven-week-old female wild-type nonagouti KK.Cg-a/a mice (lean) and agouti lethal yellow KK.Cg-Ay/J mice (obese) received food and water *ad libitum*, and either saline or ZEN (40 µg/kg) *per os* for 15 days. Body and organ weights, and estrous cyclicity were recorded, and ovaries collected posteuthanasia for protein analysis. Body and liver weights were increased ($P < 0.05$) in the obese mice, but obesity did not affect ($P > 0.05$) heart, kidney, spleen, uterus, or ovary weight and there was no impact ($P > 0.05$) of ZEN exposure on body or organ weight in lean or obese mice. Obese mice had shorter proestrus ($P < 0.05$) and a tendency ($P = 0.055$) for longer metestrus/diestrus. ZEN exposure in obese mice increased estrus but shortened metestrus/diestrus length. Neither obesity nor ZEN exposure impacted ($P > 0.05$) circulating progesterone, or ovarian abundance of EPHX1, GSTP1, CYP2E1, ATM, BRCA1, DNMT1, HDAC1, H4K16ac, or H3K9me3. Lean mice exposed to ZEN had a minor increase in γH2AX abundance ($P < 0.05$). In lean and obese mice, LC–MS/MS identified alterations to proteins involved in chemical metabolism, DNA repair and reproduction. These data identify ZEN-induced adverse ovarian modes of action and suggest that obesity is additive to ZEN-induced ovotoxicity.

Key words: zearalenone, obesity, ovary, chemical metabolism, DNA damage repair, ovarian proteome.

Introduction

The ovary performs two major roles: development of oocytes and hormone production and secretion [1–3]. Proper functioning of the ovary can be affected by exposure to xenobiotics [4–6], which can cause temporary or permanent infertility [3] or endocrine disruption [6]. Premature cessation of ovarian activity is associated with a heightened risk for development of a number of diseases in women [7–13].

Zearalenone (ZEN) is a nonsteroidal mycotoxin with estrogenic activity produced by *Fusarium* species [14–18]. Occurring naturally in warm temperatures [19], ZEN is a common contaminant in cereal crops like maize [20–23], rye [20], wheat [20, 24], barley [20, 23], but can also be detected in other dietary sources like nuts [25], flour [20], beer [20, 26], and milk [27]. Stable at high temperatures, ZEN is difficult to degrade during common food processing, becoming a public health problem [19, 28, 29]. The chemical structure of ZEN

is similar to 17β-estradiol and other natural estrogens, which allows it to bind to estrogen receptors, causing estrogenicity [16, 17], and thus, ZEN is considered an endocrine disruptor [18]. The most sensitive ZEN target is the reproductive system, but estrogen receptor-positive tissues can also be responsive [14, 16, 19, 30]. Reproductive phenotypic effects of ZEN exposure in swine include abnormal lactation [14], vulvovaginitis [14], pseudopregnancy [31], abortion [14], stillbirths [14], altered follicle stimulating hormone [30, 32], progesterone [33] and 17β-estradiol [33] and follicular impacts [34]. Rats and mice also have negative reproductive effects due to ZEN exposure including anovulation [35], altered folliculogenesis [36], persistent estrus [14], decreased fertility [37], and reduced litter size [37].

In US adults, the prevalence of female obesity is approximately 40%, and 20% in females aged 19 years and younger. Higher rates affect minority populations, especially non-Hispanic black and Hispanic women in whom 50% are obese [38]. Unsurprisingly, obesity is also an issue in developing countries [39]. In women, obesity has negative reproductive effects [40–50] including polycystic ovarian syndrome [40], decreased fecundity [41, 42], poor oocyte quality [43], increased risk of birth defects [44, 45], premature [46, 47] and stillbirth [48], and gestational diabetes [49]. Synthesis and metabolism of ovarian steroid hormones are also altered by obesity [50]. Our previous studies discovered that obesity can induce low level DNA damage [51, 52], accelerate oxidative DNA damage and oxidative stress [51], alter the phosphatidylinositol-3 kinase (PI3K) [53, 54] pathway, reduce and blunt the response of ovarian chemical metabolism proteins [53, 55] and reduce primordial follicle number [51, 55, 56]. Thus, the ovary from an obese female has apparent greater sensitivity to reproductive toxicants.

This study investigated ovarian mechanisms of ZEN-induced toxicity and also explored the hypothesis that obesity enhances ovarian sensitivity to ZEN by altering the ovarian abundance of proteins involved in chemical metabolism, DNA damage sensing and repair, and impacting serum progesterone and 17β-estradiol in female mice.

Materials and methods

Reagents

ZEN (CAS # 17924–92-4), 2-β-mercaptoethanol, phosphate-buffered saline (PBS), tris-buffered saline (TBS), nonfat dry milk, hematoxylin, eosin, tris–HCl were purchased from Sigma–Aldrich Inc (St. Louis, MO, USA). Tween 20 and glycine were purchased from Fisher Bioreagents (Fair Lawn, NJ, USA). Precast 4–20% MINI-PROTEAN TGX gels were obtained from Bio-Rad Laboratories, Inc. (Hercules, CA, USA). SignalFire ECL reagent was purchased from Cell Signaling Technology (Danvers, MA, USA). Ponceau S was obtained from Thermo Fisher Scientific (Waltham MA, USA). Restore PLUS Western Blot Stripping buffer was purchased from Thermo Scientific (Rockford, IL, USA). Primary antibodies against H4K16ac (NB21-2077), H3K9me3 (NB21-1073), HDAC1 (NB100-56340) and DNMT1 (NB100-56519) were purchased from Novus Biologicals (Centennial, CO, USA). GSTP1 (ab8902) primary antibody was purchased from Millipore (Temecula, CA, USA). ATM (ab199726), EPHX1 (ab96695) and CYP2E1 (ab28146) primary antibodies were purchased from Abcam (Cambridge, MA, USA). BRCA1 ((D-9) SC-6954) primary antibody was purchased from Santa Cruz Biotechnology, Inc. (Dallas, TX, USA). γH2AX ((Ser139) #2577) primary, goat antirabbit (7074 s) and goat antimouse (7076 s) secondary antibodies were purchased from Cell Signaling Technology (Danvers, MA, USA). Progesterone and estradiol ELISA kits were obtained from DRG International, Inc. (Springfield, NJ, USA). Pierce BCA (bicinchoninic acid assay) protein assay kit was obtained from Thermo Fisher Scientific (Rockfield, IL, USA).

Animals

All the experimental animal protocols for this study were approved by the Iowa State University Animal Care Committee. Female wild-type normal nonagouti KK.Cg-a/a, designated lean henceforth (n = 10 per group) and agouti lethal yellow KK.Cg-Ay/J, designated obese henceforth (n = 10 per group) were purchased from Jackson Laboratories (Bar Harbor, Maine) at 5 weeks of age. The mice were housed in Innovive cages with 2 or 3 animals per cage under identical controlled conditions; temperature between 21°C and 22°C, humidity of 20–30% and a light cycle of 12 h light/12 h darkness. The mice were given water and food (2014 Teklad Global 14% Protein Rodent Diet) *ad libitum*. At 7 weeks of age, the mice were dosed with saline solution as vehicle control (CT) or a ZEN solution of 40 µg/kg (0.04 ppm) per body weight for 15 days which they drank from a pipette tip. The ZEN dose was chosen based upon documented ovarian effects [36] and on the level of human exposure [19, 57]. This age of mouse was chosen because the number of primordial follicles is decreased from 12 weeks onwards in the obese mice [51, 55, 56]. Food intake (calculated as food disappearance per cage/number of mice per cage) and body weight gain were monitored twice per week.

Monitoring of estrous cycle

Vaginal cytology monitoring was performed for 14 days. Sterile plastic pipette tips were used to lavage the vagina with saline [58]. The saline solution was gently flushed 3–5 times and the final flush was collected and observed under a microscope [58]. During the proestrus stage, nucleated epithelial cells comprise the majority of cells though some cornified and leukocytes may appear [58, 59]. Large cornified cells with irregular shape and no visible or degenerated nucleus denote the estrous stage [58, 59]. In the metestrus stage, mostly leukocytes, some cornified epithelial cells, and a few nucleated epithelial cells appear [58, 59]. Finally, at the diestrus stage a predominance of polymorphonuclear leucocytes with few nucleated epithelial cells are identified [58, 59].

Tissue collection

Euthanasia and tissue collection were performed using CO_2 asphyxiation followed by cervical dislocation when mice were at the second day of the diestrus stage of the estrous cycle. Euthanasia was performed in 90% of the mice within 4 days after dosing completion. Blood samples were collected via cardiac puncture. Heart, liver, kidneys, spleen, uterus, and ovaries were collected, excess fat was trimmed from all tissues and tissues were weighed. One ovary was frozen and stored at −80°C for protein analysis.

Serum 17β-estradiol and progesterone hormone level quantification

Blood samples were centrifuged for 15 min at 10 621 rcf and 4°C. Serum was separated from red blood cells which were discarded. 17β-estradiol and progesterone in serum were quantified using ELISA kits following the manufacturer's instructions. For the progesterone (LC = 5; LZ = 5; OC = 5; OZ = 4) and 17β-estradiol (LC = 5; LZ = 5; OC = 5; OZ = 3) analyses, 19 and 18 serum samples

were analyzed with the ELISA kit respectively with two technical replicates per sample, as sufficient volume of blood was not obtained from all animals. For the 17β-estradiol assay, several samples were below the detectable range of the assay kit (LC = 2; LZ = 3; OC = 2; OZ = 2) thus, the data are not reported herein. All samples were within the analytical range of the progesterone ELISA kit.

Protein isolation

Ovaries were homogenized in lysis buffer (50 mM Tris–HCl and 1 mM EDTA (pH ~8.5)) to isolate total ovarian protein. Samples (LC = 5; LZ = 5; OC = 5; OZ = 5); were centrifugated at 10 621 rcf for 15 min twice and the supernatant was collected each time. Protein concentration was measured using the BCA assay. Absorbance values were detected at 560 nm by an Eon Microplate Spectrophotometer (Bio-Tek Instruments Inc. Winooski, VT, USA).

Western blot analysis

Protein (7 µg) was separated on MINI-PROTEAN TGX gels for 15 min at 60 V followed by 1 h at 100 V. Protein (LC = 3; LZ = 3; OC = 3; OZ = 3) was transferred from the gel to a nitrocellulose membrane using a semidry transfer (iBlot) or by wet transfer for 1 h at 100 V in ice. Using Ponceau S staining, the total amount of proteins transferred in each lane was recorded. A solution of 5% nonfat dried milk with 1× PBST (semidry transfer) or 1× TBST (wet transfer) was used to incubate the membrane for 1 h at room temperature to reduce nonspecific binding. Primary antibodies were added, and membranes were incubated overnight. Primary (H4K16ac—1:200, H3K9me3—1:200, HDAC1—1:100, DNMT1—1:200, ATM—1:100, GSTP1—1:2500, EPHX1—1:500, CYP2E1—1:500, BRCA1—1:100 and γH2AX—1:100) and secondary (1:2000–1:5000) antibody solutions were prepared with 5% nonfat dried milk with 1× PBST or 1× TBST. After this incubation, membranes were washed three times for 10 min each with 1× PBST or 1× TBST and incubated with secondary antibodies at room temperature for 1 h. After incubation with secondary antibodies, the membranes were washed repeating the steps above followed by a 7 min incubation period with ECL SignalFire reagent. X-ray film exposure was performed in the darkroom. Densitometric analysis was performed using Image J software (NCBI). All of the samples for each specific protein were run on the same gel. Specific protein levels were normalized to Ponceau S staining of total protein to account for any discrepancy in loading efficiency.

LC–MS/MS proteome analysis and gene ontology analysis

Liquid chromatography–tandem mass spectrometry (LC–MS/MS) analysis was performed as previously described [60]. Briefly, total protein samples (LC = 5; LZ = 5; OC = 5; OZ = 5) were digested with trypsin/Lys-C for 16 h, dried down and reconstituted in buffer A (47.5 µL, 0.1% formic acid/water. Peptide Retention Time Calibration (PRTC) was spiked into each sample as an internal control. Protein samples and PRTC were injected onto a LC column to be separated and analyzed with a mass spectrometer. Theoretical fragmentation patterns from MASCOT or Sequest HT were used to compare the fragmentation patterns and intact results to identify peptides. The areas of the top three unique peptides were used to identify the proteins. Only proteins that had three peptide hits within samples and that were identified in all samples were considered for analysis. Uniprot identifiers were used to obtain biological, molecular and pathway information of each protein. For gene ontology (GO) analysis PANTHER version 15.0 software was used. All samples with $P < 0.05$ were compared to the *Mus musculus* reference list to obtain pathways in which altered proteins are involved.

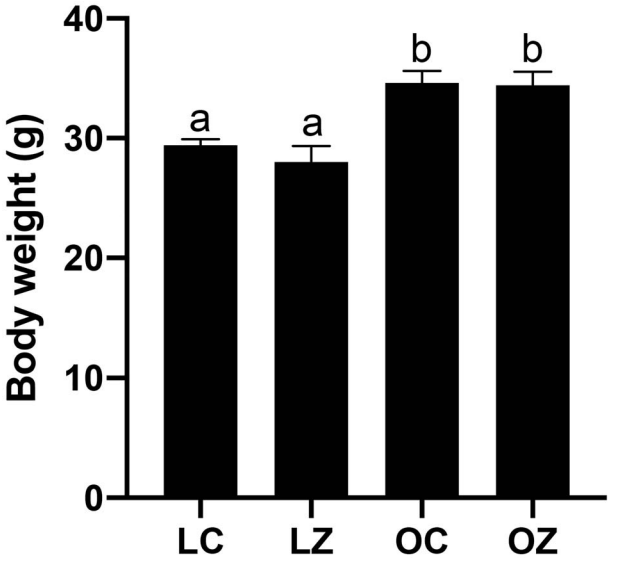

Figure 1. Impact of obesity and ZEN exposure on body weight. Mice were weighed prior to euthanasia. Bars represent body weight (g) ± SEM. Superscript letters indicate significant differences; $P < 0.05$; $n = 5$/treatment. Lean control-treated mice = LC; lean zearalenone-exposed mice = LZ; obese control-treated mice = OC; obese zearalenone-exposed mice = OZ.

Statistical analysis

Statistical analyses were performed using GraphPad Prism 8.4.1 software. For comparisons of two treatments (i.e. LC vs. LZ; OC vs. OZ; LC vs. OC), unpaired *t*-tests without adjustments were used. Two-way analysis of variance (two-way ANOVA) was performed to compare two independent variables (body composition and ZEN exposure) using Tukey's multiple comparison test. A *P* value ≤0.05 was defined as a statistically different result between treatments.

Results

Effects of ZEN exposure and obesity on food intake and body weight

Lean and obese genotype mice were weighed before starting oral administration of saline solution (CT) or ZEN. There was no difference in food intake ($P > 0.05$) due to ZEN exposure, however, as anticipated, mean food intake for the obese was higher compared to the lean mice (LC = 67.8 ± 0.7 g; LZ = 67.4 ± 1.7 g; OC = 79.4 ± 0.25 g; OZ = 70.4 ± 5.3 g; data not shown). Body weight was monitored twice per week for the 15 days of dosing duration and increased over time in all groups (data not shown). The obese genotype mice weighed more ($P < 0.05$) than their lean genotype counterparts at the completion of the experiment (mean body weight: LC = 28.3 ± 0.5 g; LZ = 27.1 ± 1.3 g; OC = 33.0 ± 1.0 g; OZ = 32.9 ± 1.2 g; Figure 1). ZEN exposure did not impact mean body weight gain in either lean or obese mice ($P > 0.05$).

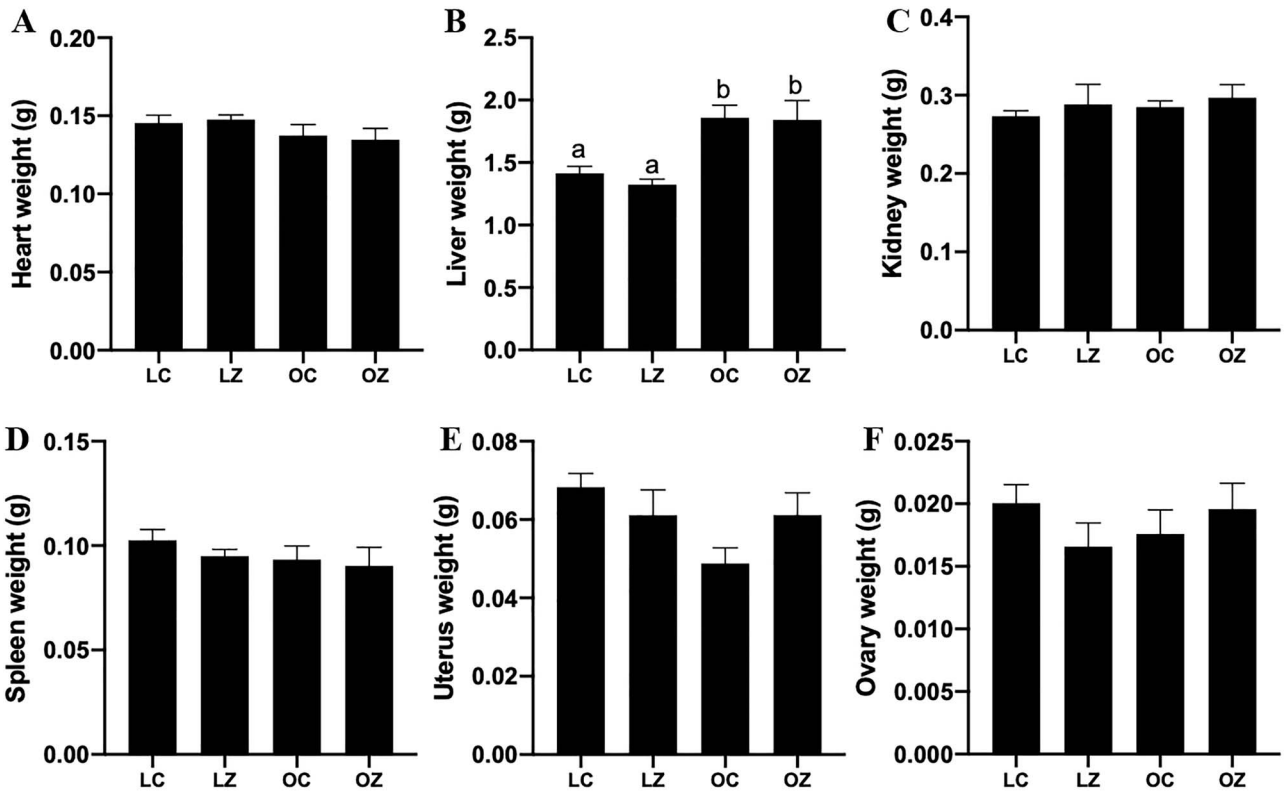

Figure 2. Effect of obesity or ZEN exposure on organ weight. After euthanasia, (A) heart, (B) liver, (C) kidney, (D) spleen, (E) uterus, and (F) ovary were collected and weighed (g). Bars represent mean weight ± SEM. Superscript letters indicate statistical difference; $P < 0.05$; $n = 5$/treatment. Lean control-treated mice = LC; lean zearalenone-exposed mice = LZ; obese control-treated mice = OC; obese zearalenone-exposed mice = OZ.

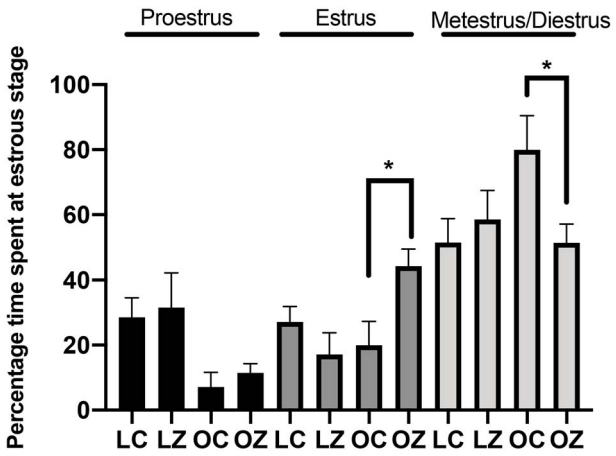

Figure 3. Estrous cyclicity impacts of obesity and ZEN exposure. The number of days at each stage of the estrous cycle were calculated over a 14-day period and presented as a percentage. Bars represent percentage of d at proestrus (black bars), estrus (dark gray bars), and metestrus + diestrus (light gray bars) ± SEM. Asterix indicates differences between treatments; $P < 0.05$; $n = 5$/treatment. Lean control-treated mice = LC; lean zearalenone-exposed mice = LZ; obese control-treated mice = OC; obese zearalenone-exposed mice = OZ.

Effects of obesity and ZEN exposure on organ weight

Mean hepatic weight was greater ($P < 0.05$) in the obese relative to lean mice (Figure 2B; LC = 1.4 ± 0.05 g; LZ = 1.3 ± 0.04 g; OC = 1.9 ± 0.1 g; OZ = 1.8 ± 0.13 g). The livers of the obese group also appeared visually paler compared to the lean group. There were no impacts of obesity or ZEN exposure on mean weights of heart (Figure 2A), kidney (Figure 2C), spleen (Figure 2D), uterus (Figure 2E), or ovaries (Figure 2F).

Effects of obesity and ZEN exposure on estrous cyclicity and ovarian steroid hormone levels

Vaginal cytology was performed on each of the mice for 14 consecutive days over the dosing period to determine the effects of ZEN exposure, obesity and any additive impact of obesity and ZEN exposure on time spent at stages of the estrous cycle. Obese mice spent less time at proestrus ($P < 0.05$) and tended to spend more time in the metestrus/diestrus ($P = 0.055$) stage than the lean mice (Figure 3). The length of time spent at the estrus stage was increased ($P < 0.05$) in the obese mice treated with ZEN compared to the CT-treated obese group (Figure 3). There was also an additive impact of obesity on ZEN-induced alteration to the time spent in metestrus/diestrus which was decreased ($P < 0.05$; Figure 3). There was no observable impact ($P > 0.05$) of ZEN exposure or obesity on circulating progesterone (Figure 4). The level of circulating progesterone as measured by ELISA was in the published range for mice in the diestrus phase of the estrous cycle using ELISA as a quantification method [61].

Effects of obesity and ZEN exposure on abundance of ovarian proteins involved in chemical biotransformation

Western blotting was performed to quantify the impact of ZEN exposure, obesity or an additive effect of obesity with ZEN exposure on ovarian protein abundance of proteins involved in chemical

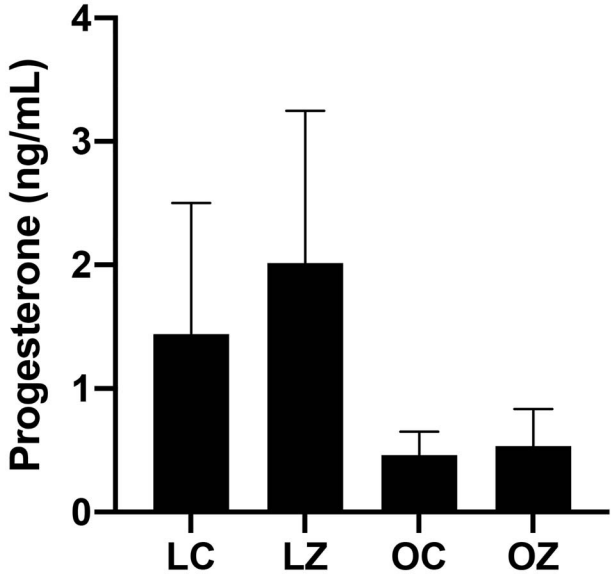

Figure 4. Ovarian steroid hormone effects of obesity and ZEN exposure. Circulating progesterone was measured by ELISA in lean control-treated mice = LC; lean zearalenone-exposed mice = LZ; obese control-treated mice = OC; obese zearalenone-exposed mice = OZ. Bars represent mean concentration ± SEM.

metabolism. There was no difference ($P > 0.05$) between any of the treatments on ovarian protein abundance of EPHX1 (Figure 5A), GSTP1 (Figure 5B) or CYP2E1 (Figure 5C).

Impact of obesity and ZEN exposure on ovarian proteins involved in DNA repair

The ovarian protein abundance of ATM, γH2AX, BRCA1, DNMT1, HDAC1, H4K16ac, and H3K9me3 were quantified via western blotting. There was no impact ($P > 0.05$) of ZEN exposure, obesity or an additive effect of obesity and ZEN exposure on ovarian protein abundance of ATM (Figure 6A), BRCA1 (Figure 6C), DNMT1(Figure 6D), HDAC1 (Figure 6E), H4K16ac (Figure 6F), and H3K9me3 (Figure 6G). However, ovarian γH2AX protein abundance was increased in lean mice treated with ZEN ($P < 0.05$) but not in obese mice (Figure 6B). γH2AX protein was also higher ($P < 0.05$) in obese CT relative to lean CT mice.

Effects of ZEN and obesity on the global ovarian proteome

LC–MS/MS proteome analysis was performed to compare protein abundance in CT and ZEN-exposed mouse ovaries and to determine if obesity altered the ovarian proteomic response to ZEN exposure. In lean mice, exposure to ZEN altered 177 proteins ($P < 0.05$). Of these, 72 were decreased and 105 were increased (Figure 7A and Supplemental Table 1). Pathway analysis was performed using PANTHER. Exposure to ZEN in the lean mice altered "5-hydroxytryptamine degradation", "angiogenesis", "apoptosis signaling pathway", "arginine biosynthesis", "DNA replication", "de novo purine biosynthesis", "dopamine receptor mediated signaling pathway", "glycolysis", "gonadotropin-releasing hormone receptor pathway", "inflammation mediated by chemokine and cytokine signaling pathway", "pentose phosphate pathway", "ras pathway", "toll receptor signaling pathway", "ubiquitin proteasome pathway", "vitamin D metabolism and pathway", "Wnt signaling pathway", "p53 pathway feedback loops 2", and "p53 pathway".

A total of 58 proteins were altered in the obese mice exposed to ZEN ($P < 0.05$). Twenty-seven proteins were decreased, and 31 proteins increased (Figure 7B and Supplemental Table 2). In the obese group, exposure to ZEN targeted the following pathways "5-hydroxytryptamine degradation", "alzheimer disease-presenilin pathway", "angiogenesis", "angiotensin II-stimulated signaling through G proteins and beta-arrestin", "apoptosis signaling pathway", "asparagine and aspartate biosynthesis", "axon guidance mediated by semaphorins", "CCKR signaling map", "cadherin signaling pathway", "cytoskeletal regulation by Rho GTPase", "gonadotropin-releasing hormone receptor pathway", "heterotrimeric G-protein signaling pathway-Gq alpha and Go alpha mediated pathway", "huntington disease", "inflammation mediated by chemokine and cytokine signaling pathway", "integrin signaling pathway", "parkinson disease", "proline biosynthesis", "ras pathway", and "vitamin D metabolism and pathway".

Obesity alone altered 406 ovarian proteins ($P < 0.05$); 233 were increased and 173 were decreased (Figure 7C and Supplemental Table 3). In the obese group, pathways altered were: "5-hydroxytryptamine degradation", "DNA replication", "angiogenesis", "gonadotropin-releasing hormone receptor pathway", "CCKR signaling map", "JAK/STAT signaling pathway", "oxidative stress response", "p53 pathway", "p53 pathway feedback loops2", "mRNA splicing", "Wnt signaling pathway", "vitamin D metabolism and pathway", "TCA cycle", "ras pathway", "pyruvate metabolism", and "inflammation mediated by chemokine and cytokine signaling pathway".

Discussion

Dietary exposure of humans and animals to ZEN is widespread, and dependent on climate conditions since inadequate drying of grains can increase the incidence of ZEN contamination. Exposure to ZEN has reproductive effects in females [14, 16, 19] and this study had two major objectives: the first was to determine modes of action of ZEN on ovarian function and the second was to investigate if obesity influenced ZEN-induced ovarian toxicity.

The mean dietary intake of ZEN in the US has been estimated as 30 ng/kg and 20 ng/kg for Canada, Denmark, and Norway [20]. In 2000, the Food and Agriculture Organization of the United States/-World Health Organization Expert Committee on Food Additives established a provisional maximum tolerable daily intake (PMTDI) of 0.5 μg/kg [57]. The PMTDI was established based on ZEN and metabolites estrogenic activity in pigs, the most sensitive species to ZEN [57]. The European Food Safety Authority Panel (EFSA) on Contaminants in the Food Chain established a tolerable daily intake (TDI) for ZEN of 0.25 μg/kg after evaluating food samples and grains from 19 European countries in the period between 2005 and 2010 [19]. This study found that 0.4–17% of the total dietary exposure of ZEN in adults and 0.1–5.1% in toddlers resulted from breakfast cereal consumption [19]. EFSA estimated the range of dietary ZEN exposure as between 4 and 50 ng/kg body weight per day and that chronic dietary exposure was higher among young people [19].

We chose a model of hyperphagia-induced obesity in which mice overeat until they become corpulent. Their lean counterparts consume the same food composition but eat fewer calories and are of the same genetic background. This model has altered circulating blood glucose and insulin [62], reduced primordial follicle number [51], alterations to steroidogenesis [56], and a blunted response to a

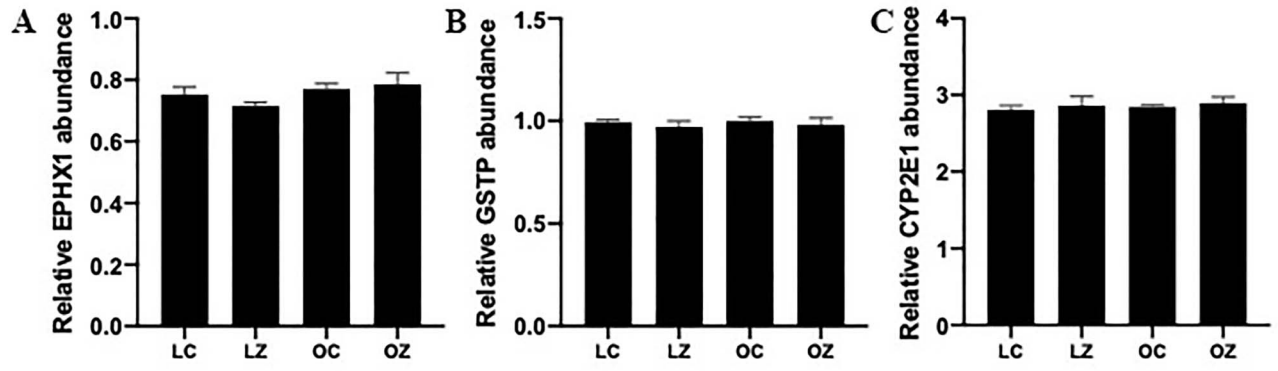

Figure 5. Impact of obesity and ZEN exposure on ovarian proteins involved in chemical biotransformation. Total ovarian protein homogenates were analyzed for (A) EPHX1, (B) GSTP, or (C) CYP2E1 protein abundance. Bars represent mean values relative to total protein staining ± SEM; $n = 3$/treatment. Lean control-treated mice = LC; lean zearalenone-exposed mice = LZ; obese control-treated mice = OC; obese zearalenone-exposed mice = OZ.

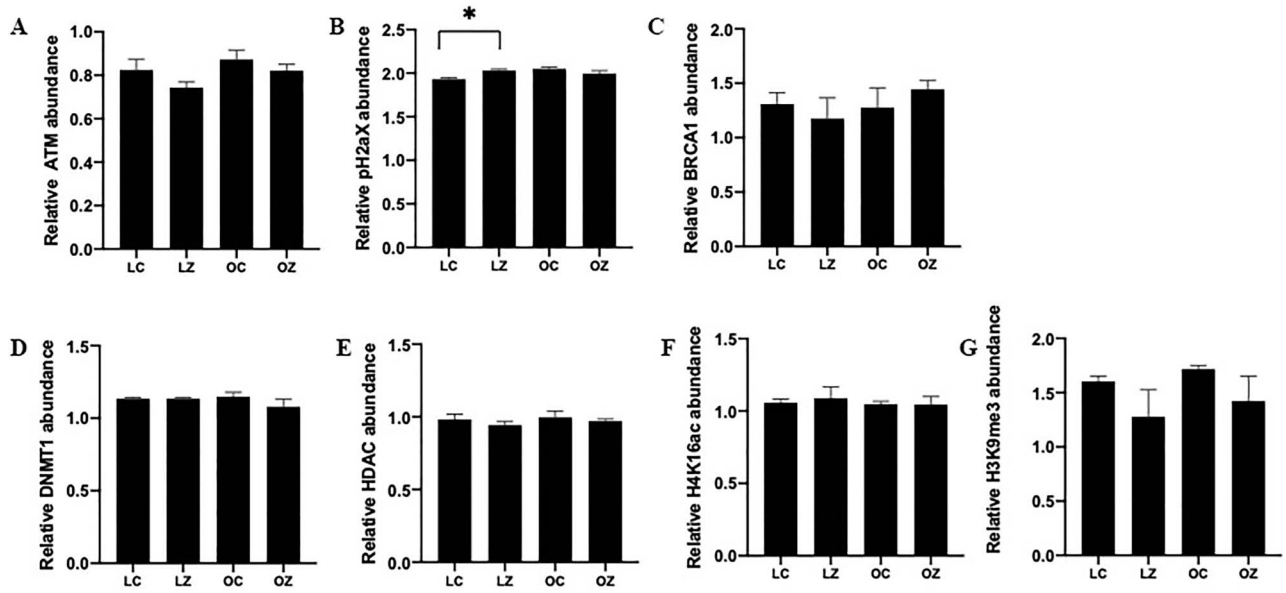

Figure 6. Impact of obesity and ZEN exposure on ovarian proteins involved in DNA repair. Total ovarian protein homogenates were analyzed for (A) ATM, (B) γH2AX (C) BRCA1, (D) DNMT1, (E) HDAC1, (F) H4K16ac, and (G) H3K9me3. Bars represent mean values relative to total protein staining ± SEM. Asterix indicates differences between treatment; $P < 0.05$; $n = 3$/treatment. Lean control-treated mice = LC; lean zearalenone-exposed mice = LZ; obese control-treated mice = OC; obese zearalenone-exposed mice = OZ.

chemical challenge [51]. Exposure began when mice were 7 weeks of age, chosen so that there was not a difference in ovarian follicle composition at the onset of dosing. Lean and obese mice were exposed to 40 µg/kg (0.04 ppm) body weight of ZEN for 15 days, and this exposure was based upon a study in which exposure to ZEN affected meiotic progression and induced DNA double-strand breaks, altered oocyte cyst breakdown and primordial follicle formation [36], albeit in a different mouse strain.

There are conflicting reports on the impact of ZEN exposure on body weight gain. There was no effect of ZEN exposure on average daily body weight gain in prepubertal gilts [63]. There are studies, however, on ZEN exposure in which reduced body weight has been noted as a phenotypic impact. Two studies performed in rats noted decreased food intake due to ZEN exposure [64, 65]. In mice exposed to either 10 ppm of ZEN plus 5 ppm deoxynivalenol (DON; another mycotoxin produced by *Fusarium* species [66]), or 25 ppm DON decreased food intake was observed [67]. Administration via feeding of different doses of ZEN (0.088–0.358 mg/kg) to gilts decreased mean daily weight gain [68], and three ZEN exposure studies in rats documented decreased body weight gain [64, 65, 69], which was dose (1–50 mg/kg) and developmental stage dependent (nonpregnant or pregnant) [64, 65, 69]. A chronic ZEN exposure (50 or 100 mg/kg) study in mice (both male and female) for 103 weeks determined that ZEN decreased mean body weight gain in both biological sexes [69]. Further, another finding of decreased body weight in mice exposed to DON, was ameliorated by addition of dietary ZEN (10 mg/kg of ZEN + 5 mg/kg of DON) [67]. In contrast to all of these findings, is a study in which ZEN (1.8 mg/kg) exposure increased body weight in exposed rats [70].

Food intake and weight gain were monitored during the study, to confirm that the obese strain reached a greater final body weight and to determine if ZEN exposure altered food intake, potentially acting as an obesogen. As per experimental design, the obese strain mice had higher food intake and a subsequent higher final body weight.

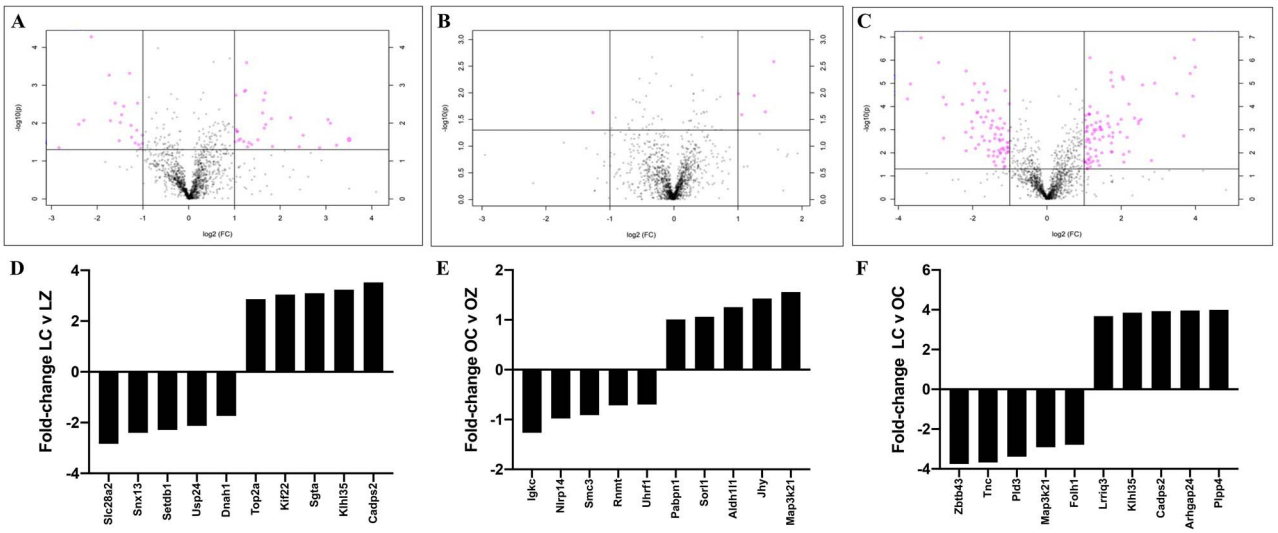

Figure 7. Ovarian protein identification and quantification via LC–MS/MS. Total ovarian protein homogenates were analyzed by LC–MS/MS and bioinformatic comparison performed between peptides identified in (A) LC vs. LZ, (B) OC vs. OZ, and (C) LC vs. OC. Pink dots above the solid horizontal line indicate increased (upper right corner) or decreased (upper left corner) proteins; $n = 5$/treatment; $P < 0.05$. The top-five increased and decreased proteins per comparison are illustrated as fold-change in (D) LC vs, LZ, (E) OC vs. OZ, and (F) LC vs. OC treated mice.

Importantly, exposure to ZEN did not affect food intake or body weight of lean mice. These findings thus eliminate any confounding effect of reduced or increased food intake or body weight on the molecular findings in this study and reduce the likelihood that ZEN influences obesity by stimulating higher food intake.

In this study, there was no difference in the organ weight within groups due to exposure to ZEN. Liver weight in the obese mice was higher compared to the lean genotype, a finding that has been previously documented [51]. Similar to our findings, chickens exposed to a single oral dose of ZEN (15.0 g/kg) had no impact on liver, oviduct or comb weight [71]. On the other hand, organ weight impacts of ZEN have been noted in other species. Both male and female rats exposed to 1.25 or 3.75 mg/kg body weight of ZEN for 8 or 10 weeks had enlarged livers and in male rats, the adrenal glands and spleens were larger [72]. Female rats that were fed for 14 days with 250 µg/g had enlarged kidney and liver but no effect on uterine weight [73]. Chickens exposed to ZEN orally and intramuscularly (50, 200, 400, and 800 mg/kg) for 7 days had increased oviduct weight due to both administration routes [71]. In addition, intramuscular ZEN exposure caused increased liver and comb weight [71]. ZEN exposure caused uterine enlargement in Yorkshire gilts who received doses of 10, 20, or 40 µg/g for 4 weeks [73]. Furthermore, female pigs exposed to 1.1 mg/kg of ZEN for 24 or 28 days had increased reproductive tract weight [74, 75]. Gilts fed diets containing 1.1, 2.0, and 3.2 mg/kg of ZEN for 18 days had increased liver, kidney, and reproductive tract (ovary, uteri, and vagina) weights whereas spleen relative weight was decreased in a dose-dependent manner [76]. The current study did not note any ZEN-induced alterations to organ weight, again emphasizing that overt toxicity was absent, and suggesting a dose- and species-dependent impact of ZEN.

Days spent in the estrus stage were increased whereas days spent at metestrus/diestrus stages decreased in the ZEN-exposed obese but not lean mice, suggesting enhanced sensitivity of the obese mice to ZEN exposure. Obesity also altered estrous cyclicity with the obese mice having a shortened proestrus stage but lengthened metestrus/diestrus stage. It is known that obesity can impact the estrous cycle causing a decrease in the length of the estrus stage and an increase in the days spent at the diestrus stage [53]. Additionally, ZEN can cause changes in the estrous cyclicity depending on the time of administration and dose [77]. Gilts provided 200 µg/kg body weight of ZEN for 8 days had false estrus indications on day 4 of treatment [78]. Longer interestrus periods were observed in gilts fed with 5 and 10 ppm of ZEN during day 5–20 of the estrous cycle [79]. Lengthened estrous cyclicity was noted in gilts exposed to 20 mg of ZEN on days 6–10 and days 11–15 of the estrous cycle [80]. Within 50 days after puberty, no behavioral estrus was detected in 45% of gilts fed with a diet containing 3.61 ppm of ZEN [31]. These findings indicate that exposure to ZEN alters estrous cyclicity in a variety of species including swine and mice.

There was no impact of obesity or ZEN exposure on circulating progesterone. Several samples were below the detectable range of the 17β-estradiol assay kit, most likely due to blood being collected during diestrus. Progesterone was lower numerically in the obese mice but the high level of variability in the lean mice precluded statistical difference being apparent. Thus, despite observable alterations to the estrous cycle stage lengths due to both obesity and ZEN exposure in obese mice, this was not reflected by a change in the major ovarian hormone, progesterone, in circulation at the stage of the estrous cycle at which the ovaries were collected. Pregnant Sprague–Dawley rats were exposed to a daily dose of 1–8 mg/kg ZEN from gestation day 6 to 19 [65] and 17β-estradiol and progesterone levels were decreased in a dose-dependent manner beginning at 2 mg/kg [65]. Prepubertal pigs exposed to 238.5 µg/kg ZEN for 24 days and then to 20 or 40 µg/kg ZEN for 48 days had no impact on 17β-estradiol level, which could be attributable to their prepubertal status [81, 82]. In postpubertal pigs progesterone concentrations were increased due to ZEN exposure (20 mg on days 6–10 or days 11–15 of the estrous cycle) [80]. Further, pigs fed 60 or 90 mg/kg ZEN at 2, 3, and 6 weeks postbreeding had decreased circulating progesterone and at 4 weeks postbreeding 17β-estradiol was also decreased [83]. Considering the low ZEN exposure level used in the current study, it is perhaps not surprising that endocrine disruption was not evident. It would also be a consideration for the future to collect ovaries at an estrous cycle stage more appropriate for quantification of 17β-estradiol effects.

Total ovarian protein abundance of xenobiotic biotransformation enzymes (GSTP, CYP2E1, and EPHX1), as well as proteins involved in DNA damage repair (ATM, γH2AX, BRCA1, DNMT1, HDAC1, H4K16ac, and H3K9me3) was investigated. Surprisingly, there was no difference in the ovarian protein abundance of EPHX1, CYP2E1, GSTP, ATM, BRCA1, DNMT1, HDAC1, H4K16ac, or H3K9me3 due to either obesity or ZEN exposure. Interestingly, the gold standard marker of DNA double-strand breaks, γH2AX was slightly increased in the lean mice treated with ZEN, but not in the obese group, supporting that ZEN may induce genotoxicity in the ovary as a mode of action. The level of γH2AX increase is very minor and whether this is of biological significance remains unclear. Other studies have determined that ZEN exposure alters γH2AX and BRCA1 expression, and other proteins related to DNA double-strand breaks and repair [36, 84]. At the diplotene stage of meiosis γH2AX staining as well as mRNA abundance of *Mlh1*, *Rad51*, and *Brca1* were increased in mice treated with 20 µg/kg of ZEN [36] and mice treated with 10 and 30 µM of ZEN had increased γH2AX positive ovarian cells [84]. Our finding of increased γH2AX, therefore, albeit a small increase, recapitulates findings of other studies on the ovarian effects of ZEN exposure. Lack of γH2AX increase in ovaries of obese mice could indicate alterations to ZEN-induced genotoxicity or an altered protein response to DNA double-strand break in the ovary of the obese mice.

Proteomic profiling can provide important insights into the impact of a toxic exposure on cellular function. Since the aim of the study was to identify modes of action of ZEN exposure in lean and obese mice, ovaries were collected at the same stage of the estrous cycle on the second day of diestrus. In choosing this strategy, it is acknowledged that a lag time from the cessation of dosing to tissue collection exists but minimizing hormonal milieu variation was considered an important aspect of the data interpretation. Using LC–MS/MS, alterations to the protein profile were identified in three specific treatment comparisons: lean CT vs. lean ZEN, obese CT vs. obese ZEN, and lean CT vs. obese CT. Altered ovarian abundance of proteins involved in DNA damage and repair, chemical metabolism, and reproduction were consistently discovered in the ovaries of ZEN-exposed mice, with treatment effects as expanded upon below.

Proteomics analysis identified that GSTP1 ovarian protein abundance was increased in the lean mice exposed to ZEN and due to obesity. The biological and molecular functions of this protein are related to drug binding [85], xenobiotic metabolism process [85], and response to toxic substances [85]. With this finding, it is important to keep in mind that it is known that LC–MS/MS is a more sensitive technique compared to western blot, and that could be the reason that altered abundance of GSTP1 was determined by LC–MS/MS but not using western blotting. Ovarian protein abundance of EPHX2 was also altered due to obesity, and due to ZEN exposure in lean mice, but in opposing directions in both. EPHX2, as well as EPHX1, is an epoxide hydrolase involved in the metabolism of chemicals [86–88]. Epoxide hydrolases are divided into two groups: microsomal epoxide hydrolase (EPHX1) and soluble cytosolic epoxide hydrolase (EPHX2) [89–92]. Interestingly, ras homolog family member A (RHOA) is a protein whose ovarian abundance was decreased by basal obesity and by ZEN exposure in lean mice, but was increased by ZEN exposure in obese mice. RHOA is part of the Rho GTPase family, and it is important for certain cell functions such as migration and survival [93], gene expression [93], and cell division [93]. A response to drug [85], glucose [85], and ethanol [85] is also considered a biological function of RHOA. These proteins are all involved in the metabolism of chemicals, and changes in the ovarian abundance due to obesity suggests that in this study, as in others from our group [53–55], that obesity alters the basal ovarian capacity for chemical biotransformation. In addition, these findings provide additional information on ovarian ZEN chemical biotransformation and the impact of obesity on xenobiotic metabolism.

Proteins that are involved in DNA damage repair were also identified to be altered by either ZEN or obesity. Exposure to ZEN in lean mice reduced RPS27L and UBE2N, but increased CUL4A, USP47, TOP2A, KIF22. Ribosomal protein S27 like (RPS27L) regulates P53 activity [94], which functions in cell survival and is activated by DNA damaging agents [95]. Ubiquitin conjugating enzyme E2 N (UBE2N) is involved in regulation of innate immune signaling [96], glycolysis [96], cell survival [96], RNA splicing [96], and the DNA damage response [96]. Kinesin family member 22 (KIF22) plays an important role in mitosis and it is part of kinesin superfamily proteins that have been associated with carcinogenesis and cancer progression [97]. Exposure to ZEN in lean mice reduced abundance of PPP1R12A, CCT2, RHOA, and TUFM and increased HSPA5, GSTP1, AKR7A2, USP47, BLMH, SCFD1, and TOP2A level. Protein phosphatase 1 regulatory subunit 12A (PPP1R12A) is associated with alterations in the PI3K/AKT pathway and is a tumor suppressor with a proposed role in cancer chemoresistance [98]. DNA topoisomerase II alpha (TOP2A) has an important role in DNA replication [99], response to DNA damage stimulus [85], and drug binding [85] and is increased by ZEN exposure.

Related to reproductive function, HSP90AA1, GPI, CA2, CTNNB1, and STRA6 were increased whereas NSD1, MGARP, and OXCT1 were decreased by ZEN exposure. Nuclear receptor-binding SET domain protein 1 (NSD1) is part of histone lysine methyltransferases family [100, 101], with a molecular function related to estrogen receptor-binding [101]. Signaling receptor and transporter of retinol STRA6 (STRA6) regulates cellular uptake of vitamin A [102], is present in the reproductive organs [103] and placenta [103] and has been associated with activation of JAK–STAT pathway [104, 105] and insulin signaling [106]. Thus, ZEN exposure in lean mice altered ovarian proteins involved in xenobiotic metabolism, DNA repair and reproductive function.

In obese mice exposed to ZEN, DNA damage repair proteins increased were DDX5, RUVBL1, and ACTR2 whereas SMC3, UHRF1, and HSPA1A were decreased in abundance, again supporting that ZEN induces ovarian DNA damage but that the ovarian response differs to that of the lean mice. Structural maintenance of chromosomes protein 3 (SMC3) is part of a protein complex that is important for DNA repair [85, 107] and regulation of gene expression [107]. Actin related protein 2 (ACTR2) is part of the ARP2/3 complex that is required for cell migration [108], regulation of actin filament nucleation [109] and organization in the cytoplasm [110, 111], and double-strand breaks involved in DNA damage and repair [85, 112]. RAN binding protein 1 (RANBP1) can control mitotic microtubules function that can be a target for chemotherapeutic drugs [113], and its biological process is associated with cellular response to drugs [85]. The altered ovarian protein abundance related to chemical metabolism were RHOA, ACTR2, ANXA1, NAMPT, CCT7, and EPHX2 which were increased in abundance whereas RANBP1 and CCT3 were lower in ovaries of obese ZEN-exposed mice. Thus, there is strong evidence for the involvement of RHOA and EPHX2 in the ovarian response to ZEN in both lean and obese mice. Finally, in the group of proteins related to reproduction, two proteins with an identified reproductive function were increased—ANXA1 and AKR1C18. Annexin A1 (ANXA1) is abundantly expressed in many tissues

including testis [114], ovaries [115], and placenta [115, 116], and regulates steroid hormone secretion [117], and ANXA1 is elevated during pregnancy [116, 118]. Other biological processes in which ANXA1 is involved are estrous cyclicity [117], prolactin secretion [85], response to estradiol [85], and response to drugs [85]. Taken together, these findings support that ZEN exposure also alters DNA repair, chemical metabolism, and proteins involved in reproduction in the ovary but there is differential protein abundance between the ovaries from lean and obese mice.

Obesity in the absence of ZEN exposure altered proteins with potential important ovarian function. Uveal autoantigen with coiled-coil domains and ankyrin repeats (UACA) regulates apoptotic pathways and is associated with DNA damage [119]. SMC3 was considerably increased by obesity. Tenascin C (TNC) and fibronectin have involvement in the extracellular matrix (ECM) and bind to integrins at the cell surface [120]. These have importance as ECM regulates synaptic transmission, and cell signaling, and its expression and activity can be controlled by chemicals [120]. Gamma-aminobutyric acid type A receptor subunit alpha4 (GABRA4) is a $GABA_A$ receptor that is expressed in glial cells and neurons and is involved in neurotransmission processes [121]. The alpha4 and alpha6 subunits have extrasynaptic localization, and are altered by xenobiotic exposure including benzodiazepines [121], alcohol [121], and drugs of abuse [121]. Related to reproduction, hexosaminidase subunit beta (HEXB) has an important role in the central nervous system and breaks down sphingolipids, oligosaccharides, and glycoproteins [122]. It has been associated with reproduction [123], fertility rates [85, 123], and oogenesis [85]. Serpin family F member 1 (SERPINF1) encodes the pigment epithelium-derived factor (PEDF) [124], an inhibitor of angiogenesis [125], and regulator of bone density [126]. Alterations in PEDF levels are associated with cancer [127], ovarian hyperstimulation [127], endometriosis [127], and diabetes [127]. Thus, in the absence of chemical exposure, obesity alone alters ovarian protein abundance in manners that could contribute to altered fertility and sensitivity to chemical exposure.

It is recognized that ZEN can act in an estrogenic manner by binding the estrogen receptors [128]. Thus, we interrogated our proteomics findings manually by searching the literature for links between estrogen signaling and proteins that were altered in abundance in our LC–MS/MS experiments. We determined that RHOA [129, 130], GSTP1 [131], NSD1 [101], SMC3 [132], ANXA1 [133], TCN [134], GABRA4 [135], PEDF [136], and TOP2A [137] are associated with estrogen receptor activity, whereas STRA6 gene expression is regulated by progesterone receptor [138]. Thus, the exposure to ZEN in this study altered proteins that are linked with estrogen signaling, supporting an estrogenic impact of ZEN.

In conclusion, both obesity and/or ZEN exposure altered liver weight, affected the estrous cycle, increased a marker of DNA damage and repair, and proteomics analysis revealed changes in ovarian abundance of proteins related to DNA damage repair, chemical metabolism and reproduction. Taken together, the data identify ZEN-induced ovarian alterations and support that ovarian response to ZEN exposure is different in obese relative to lean mice. These findings raise concerns about how an altered physiological status can influence the effects of ovarian xenobiotic exposure.

Supplementary material

Supplementary material is available at *BIOLRE* online.

Data availability statement

Data available on request.

References

1. Hoyer PB. 11.16—Female reproductive toxicology. In: McQueen CA (ed.), *Comprehensive Toxicology*, 2nd ed. Oxford: Elsevier; 2010: 339–345.
2. Senger PL. *Pathways to pregnancy & parturition*. Washington State University Research and Technology Park, Pullman WA: Current Conceptions Inc. 2012.
3. Hoyer PB, Keating AF. Xenobiotic effects in the ovary: temporary versus permanent infertility. *Expert Opin Drug Metab Toxicol* 2014; **10**:511–523.
4. Mattison DR. Clinical manifestations of ovarian toxicity. *Reprod Toxicol* 1985; **109**:697–724.
5. Keating AF, Hoyer PB. Mechanisms of reproductive toxicity. In: *Drug Metabolism Handbook*. Hoboken, NJ: John Wiley and sons, Inc. 2009: 697–736.
6. Hoyer PB. Damage to ovarian development and function. *Cell Tissue Res* 2005; **322**:99–106.
7. Krarup T. Oocyte destruction and ovarian tumorigenesis after direct application of a chemical carcinogen (9:10-dimethyl-1:2-benzanthrene) to the mouse ovary. *Int J Cancer* 1969; **4**:61–75.
8. Krarup T. Effect of 9,10-dimethyl-1,2-denzanthracene on the mouse ovary. Ovarian tumorigenesis. *Br J Cancer* 1970; **24**:168–186.
9. Beamer WG, Tennent BJ. Gonadotropin uptake in genetic and irradiation models of ovarian Tumorigenesis1. *Biol Reprod* 1986; **34**: 761–770.
10. Tennent BJ, Beamer WG. Ovarian tumors not induced by irradiation and gonadotropins in hypogonadal (HPG) mice. *Biol Reprod* 1986; **34**:751–760.
11. Maronpot R. Ovarian toxicity and carcinogenicity in eight recent National Toxicology Program Studies. *Environ Health Perspect* 1987; **73**:125–130.
12. Hoyer PB, Sipes IG. Assessment of follicle destruction in chemical-induced ovarian toxicity. *Annu Rev Pharmacol Toxicol* 1996; **36**:307–331.
13. Hoyer PB, Devine PJ, Xiaoming Hu, Thompson KE, Sipes IG. Ovarian toxicity of 4-vinylcyclohexene diepoxide: a mechanistic model. *Toxicol Pathol* 2001; **29**:91–99.
14. Kuiper-Goodman T, Scott PM, Watanabe H. Risk assessment of the mycotoxin zearalenone. *Regul Toxicol Pharmacol* 1987; **7**:253–306.
15. Urry WH, Wehrmeister HL, Hodge EB, Hidy PH. The structure of zearalenone. *Tetrahedron Lett* 1966; **7**:3109–3114.
16. Bennett JW, Klich M. Mycotoxins. *Clin Microbiol Rev* 2003; **16**:497–516.
17. Caldwell RW, Tuite J, Stob M, Baldwin R. Zearalenone production by fusarium species. *Appl Microbiol* 1970; **20**:31–34.
18. Shier WT, Shier AC, Xie W, Mirocha CJ. Structure-activity relationships for human estrogenic activity in zearalenone mycotoxins. *Toxicon* 2001; **39**:1435–1438.
19. Chain EPoCitF. Scientific opinion on the risks for public health related to the presence of zearalenone in food. *EFSA J* 2011; **9**:2197.
20. Zinedine A, Soriano JM, Moltó JC, Mañes J. Review on the toxicity, occurrence, metabolism, detoxification, regulations and intake of zearalenone: an oestrogenic mycotoxin. *Food Chem Toxicol* 2007; **45**:1–18.
21. Caldwell RW, Tuite J. Zearalenone in freshly harvested corn. *Phytopathology* 1974; **64**:752.
22. Shotwell OL. Mycotoxins in hot spots in grains. I. Aflatoxin and zearalenone occurrence in stored corn. *Cereal chemistry* 1975; **52**: pp. 687–697.
23. Shotwell OL. *Assay Methods for Zearalenone and Its Natural Occurrence*. Park Forest South IL: Pathotox Publishers, Inc.; 1977.
24. Goyarts T, Dänicke S, Valenta H, Ueberschär K-H. Carry-over of fusarium toxins (deoxynivalenol and zearalenone) from naturally

contaminated wheat to pigs. *Food Addit Contam* 2007; **24**:369–380.
25. Poór M, Kunsági-Máté S, Bálint M, Hetényi C, Gerner Z, Lemli B. Interaction of mycotoxin zearalenone with human serum albumin. *J Photochem Photobiol B Biol* 2017; **170**:16–24.
26. Okoye ZSC. Stability of zearalenone in naturally contaminated corn during Nigerian traditional brewing. *Food Addit Contam* 1987; **4**:57–59.
27. Prelusky DB, Scott PM, Trenholm HL, Lawrence GA. Minimal transmission of zearalenone to milk of dairy cows. *J Environ Sci Health B* 1990; **25**:87–103.
28. Ryu D, Hanna MA, Bullerman LB. Stability of zearalenone during extrusion of corn grits†. *J Food Prot* 1999; **62**:1482–1484.
29. Bennett GA, Shotwell OL, Hesseltine CW. Destruction of zearalenone in contaminated corn. *J Am Oil Chem Soc* 1980; **57**:245–247.
30. He J, Wei C, Li Y, Liu Y, Wang Y, Pan J, Liu J, Wu Y, Cui S. Zearalenone and alpha-zearalenol inhibit the synthesis and secretion of pig follicle stimulating hormone via the non-classical estrogen membrane receptor GPR30. *Mol Cell Endocrinol* 2018; **461**:43–54.
31. Etienne M, Jemmali M. Effects of zearalenone (F2) on estrous activity and reproduction in gilts2. *J Anim Sci* 1982; **55**:1–10.
32. Diekman MA, Green ML, Malayer JR, Brandt KE, Long GG. Effect of zearalenone and estradiol benzoate on serum concentrations of LH, FSH and prolactin in ovariectomized gilts. *Theriogenology* 1989; **31**:1123–1130.
33. Long GG, Diekman M, Tuite JF, Shannon GM, Vesonder RF. Effect of fusarium roseum corn culture containing zearalenone on early pregnancy in swine. *Am J Vet Res* 1982; **43**:1599–1603.
34. Malekinejad H, Schoevers EJ, Daemen IJJM, Zijlstra C, Colenbrander B, Fink-Gremmels J, Roelen BAJ. Exposure of oocytes to the fusarium toxins zearalenone and deoxynivalenol causes aneuploidy and abnormal embryo development in Pigs1. *Biol Reprod* 2007; **77**:840–847.
35. Kumagai S, Shimizu T. Neonatal exposure to zearalenone causes persistent anovulatory estrus in the rat. *Arch Toxicol* 1982; **50**:279–286.
36. Liu KH, Sun XF, Feng YZ, Cheng SF, Li B, Li YP, Shen W, Li L. The impact of zearalenone on the meiotic progression and primordial follicle assembly during early oogenesis. *Toxicol Appl Pharmacol* 2017; **329**:9–17.
37. Becci PJ, Johnson WD, Hess FG, Gallo MA, Parent RA, Taylor JM. Combined two-generation reproduction-teratogenesis study of zearalenone in the rat. *J Appl Toxicol* 1982; **2**:201–206.
38. Hales CM, Carroll MD, Fryar CD, Ogden CL. Prevalence of obesity among adults and youth: United States, 2015–2016. In: *NCHS data brief*. Hyattsville, MD: National Center for Health Statistics; 2017: 8.
39. World Health O. Obesity and overweight. In: *Fact sheets*. Geneva, Switzerland: World Health Organization. vol. **2020**. 2020.
40. Pasquali R, Casimirri F. The impact of obesity on hyperandrogenism and polycystic ovary syndrome in premenopausal women. *Clin Endocrinol (Oxf)* 1993; **39**:1–16.
41. Rich-Edwards JW, Goldman MB, Willett WC, Hunter DJ, Stampfer MJ, Colditz GA, Manson JE. Adolescent body mass index and infertility caused by ovulatory disorder. *Am J Obstet Gynecol* 1994; **171**:171–177.
42. Grodstein F, Goldman MB, Cramer DW. Body mass index and ovulatory infertility. *Epidemiology* 1994; **5**:247–250.
43. Jungheim ES, Schoeller EL, Marquard KL, Louden ED, Schaffer JE, Moley KH. Diet-induced obesity model: abnormal oocytes and persistent growth abnormalities in the offspring. *Endocrinology* 2010; **151**:4039–4046.
44. Watkins ML, Rasmussen SA, Honein MA, Botto LD, Moore CA. Maternal obesity and risk for birth defects. *Pediatrics* 2003; **111**:1152.
45. Stothard KJ, Tennant PW, Bell R, Rankin J. Maternal overweight and obesity and the risk of congenital anomalies: a systematic review and meta-analysis. *JAMA* 2009; **301**:636–650.
46. McDonald SD, Han Z, Mulla S, Beyene J, on behalf of the Knowledge Synthesis Group. Overweight and obesity in mothers and risk of preterm birth and low birth weight infants: systematic review and meta-analyses. *BMJ* 2010; **341**:c3428.
47. Smith GCS, Shah I, Pell JP, Crossley JA, Dobbie R. Maternal obesity in early pregnancy and risk of spontaneous and elective preterm deliveries: a retrospective cohort study. *Am J Public Health* 2007; **97**:157–162.
48. Aune D, Saugstad OD, Henriksen T, Tonstad S. Maternal body mass index and the risk of fetal death, stillbirth, and infant death: a systematic review and meta-analysis. *JAMA* 2014; **311**:1536–1546.
49. Chu SY, Callaghan WM, Kim SY, Schmid CH, Lau J, England LJ, Dietz PM. Maternal obesity and risk of gestational diabetes mellitus. *Diabetes Care* 2007; **30**:2070–2076.
50. Pasquali R, Pelusi C, Genghini S, Cacciari M, Gambineri A. Obesity and reproductive disorders in women. *Hum Reprod Update* 2003; **9**:359–372.
51. Ganesan S, Nteeba J, Madden JA, Keating AF. Obesity alters phosphoramide mustard-induced ovarian DNA repair in mice. *Biol Reprod* 2017; **96**:491–501.
52. Ganesan S, Nteeba J, Keating AF. Enhanced susceptibility of ovaries from obese mice to 7,12-dimethylbenz[a]anthracene-induced DNA damage. *Toxicol Appl Pharmacol* 2014; **281**:203–210.
53. Nteeba J, Ganesan S, Madden JA, Dickson MJ, Keating AF. Progressive obesity alters ovarian insulin, phosphatidylinositol-3 kinase, and chemical metabolism signaling pathways and potentiates ovotoxicity induced by phosphoramide mustard in mice†. *Biol Reprod* 2017; **96**: 478–490.
54. Nteeba J, Ross JW, Perfield II JW, Keating AF. High fat diet induced obesity alters ovarian phosphatidylinositol-3 kinase signaling gene expression. *Reprod Toxicol* 2013; **42**:68–77.
55. Nteeba J, Ganesan S, Keating AF. Impact of obesity on Ovotoxicity induced by 7,12-dimethylbenz[a]anthracene in Mice1. *Biol Reprod* 2014; **90**:68.
56. Nteeba J, Ganesan S, Keating AF. Progressive obesity alters ovarian folliculogenesis with impacts on pro-inflammatory and steroidogenic signaling in female mice1. *Biol Reprod* 2014; **91**:86.
57. Joint FAOWHOECoFA, World Health O. *Evaluation of Certain Food Additives and Contaminants: Fifty-Third Report of the Joint FAO/WHO Expert Committee on Food Additives*. Geneva: World Health Organization; 2000.
58. Caligioni CS. Assessing reproductive status/stages in mice. *Curr Protoc Neurosci* 2009; **Appendix 4**:Appendix 4I.
59. Byers SL, Wiles MV, Dunn SL, Taft RA. Mouse estrous cycle identification tool and images. *PLoS One* 2012; **7**:e35538.
60. Clark KL, Talton OO, Ganesan S, Schulz LC, Keating AF. Developmental origins of ovarian disorder: impact of maternal lean gestational diabetes on the offspring ovarian proteome in mice†. *Biol Reprod* 2019; **101**:771–781.
61. Zenclussen ML, Casalis PA, Jensen F, Woidacki K, Zenclussen AC. Hormonal fluctuations during the estrous cycle modulate heme oxygenase-1 expression in the uterus. *Front Endocrinol* 2014; **5**:32.
62. Yang Z, Norwood KA, Smith JE, Kerl JG, Wood JR. Genes involved in the immediate early response and epithelial-mesenchymal transition are regulated by adipocytokines in the female reproductive tract. *Mol Reprod Dev* 2012; **79**:128–137.
63. Green ML, Diekman MA, Malayer JR, Scheidt AB, Long GG. Effect of prepubertal consumption of zearalenone on puberty and subsequent reproduction of gilts. *J Anim Sci* 1990; **68**:171–178.
64. Hueza IM, Raspantini PCF, Raspantini LER, Latorre AO, Górniak SL. Zearalenone, an estrogenic mycotoxin, is an immunotoxic compound. *Toxins* 2014; **6**:1080–1095.
65. Collins TF, Sprando RL, Black TN, Olejnik N, Eppley RM, Alam HZ, Rorie J, Ruggles DI. Effects of zearalenone on in utero development in rats. *Food Chem Toxicol* 2006; **44**:1455–1465.
66. Sobrova P, Adam V, Vasatkova A, Beklova M, Zeman L, Kizek R. Deoxynivalenol and its toxicity. *Interdisciplinary toxicology* 2010; **3**:94–99.
67. Forsell JH, Witt MF, Tai JH, Jensen R, Pestka JJ. Effects of 8-week exposure of the B6C3F1 mouse to dietary deoxynivalenol (vomitoxin) and zearalenone. *Food Chem Toxicol* 1986; **24**:213–219.

68. Alm H, Brüssow KP, Torner H, Vanselow J, Tomek W, Dänicke S, Tiemann U. Influence of fusarium-toxin contaminated feed on initial quality and meiotic competence of gilt oocytes. *Reprod Toxicol* 2006; **22**:44–50.
69. Program NT. Carcinogenesis of bioassay of zearalenone (CAS NO. 17924-92-4) IN F344/N rats and B6C3F1 mice (Feed Study). In: *Technical Report Series*. United States: National Institutes of Health; 1982: 157.
70. Denli M, Blandon JC, Salado S, Guynot ME, Pérez JF. Effect of dietary zearalenone on the performance, reproduction tract and serum biochemistry in young rats. *J Appl Anim Res* 2017; **45**:619–622.
71. Chi MS, Mirocha CJ, Weaver GA, Kurtz HJ. Effect of Zearalenone on female White leghorn chickens. *Appl Environ Microbiol* 1980; **39**:1026–1030.
72. Kiessling K-H. The effect of zearalenone on growth rate, organ weight and muscle fibre composition in growing rats. *Acta Pharmacol Toxicol* 1982; **51**:154–158.
73. James LJ, Smith TK. Effect of dietary alfalfa on zearalenone toxicity and metabolism in rats and swine. *J Anim Sci* 1982; **55**:110–118.
74. Chen Q, Lu Z, Hou W, Shi B, Shan A. Effects of modified maifanite on zearalenone toxicity in female weaner pigs. *Ital J Anim Sci* 2015; **14**:3597.
75. Jiang SZ, Yang ZB, Yang WR, Yao BQ, Zhao H, Liu FX, Chen CC, Chi F. Effects of feeding purified zearalenone contaminated diets with or without clay enterosorbent on growth, nutrient availability, and genital organs in post-weaning female pigs. *Asian-Australas J Anim Sci* 2010; **23**:74–81.
76. Jiang SZ, Yang ZB, Yang WR, Gao J, Liu FX, Broomhead J, Chi F. Effects of purified zearalenone on growth performance, organ size, serum metabolites, and oxidative stress in postweaning gilts. *J Anim Sci* 2011; **89**:3008–3015.
77. Zhang G-L, Feng Y-L, Song J-L, Zhou X-S. Zearalenone: a mycotoxin with different toxic effect in domestic and laboratory animals' granulosa cells. *Front Genet* 2018; **9**:667.
78. Zwierzchowski W, Przybyłowicz M, Obremski K, Zielonka L, Skorska-Wyszyńska E, Gajecka M, Polak M, Jakimiuk E, Jana B, Rybarczyk L, Gajecki M. Level of zearalenone in blood serum and lesions in ovarian follicles of sexually immature gilts in the course of zearalenone micotoxicosis. *Pol J Vet Sci* 2005; **8**:209–218.
79. Edwards S, Cantley TC, Rottinghaus GE, Osweiler GD, Day BN. The effects of zearalenone on reproduction in swine. I. The relationship between ingested zearalenone dose and anestrus in non-pregnant, sexually mature gilts. *Theriogenology* 1987; **28**:43–49.
80. Flowers B, Cantley T, Day BN. A comparison of effects of zearalenone and estradiol benzoate on reproductive function during the estrous cycle in Gilts2. *J Anim Sci* 1987; **65**:1576–1584.
81. Zhao L, Lei Y, Bao Y, Jia R, Ma Q, Zhang J, Chen J, Ji C. Ameliorative effects of Bacillus subtilis ANSB01G on zearalenone toxicosis in prepubertal female gilts. *Food Addit Contam* 2015; **32**:617–625.
82. Gajęcka M, Rybarczyk L, Zwierzchowski W, Jakimiuk E, Zielonka L, Obremski K, Gajęcki M. The effect of experimental, long-term exposure to low-dose zearalenone mycotoxicosis on the histological condition of ovaries in sexually immature gilts. *Theriogenology* 2011; **75**:1085–1094.
83. Long GG, Diekman MA. Effect of purified zearalenone on early gestation in gilts. *J Anim Sci* 1984; **59**:1662–1670.
84. Zhang GL, Sun XF, Feng YZ, Li B, Li YP, Yang F, Nyachoti CM, Shen W, Sun SD, Li L. Zearalenone exposure impairs ovarian primordial follicle formation via down-regulation of Lhx8 expression in vitro. *Toxicol Appl Pharmacol* 2017; **317**:33–40.
85. UniProt Consortium. UniProt: a worldwide hub of protein knowledge. *Nucleic Acids Res* 2019; **47**:D506–D515.
86. Oesch F. Mammalian epoxide hydrases: inducible enzymes catalysing the inactivation of carcinogenic and cytotoxic metabolites derived from aromatic and Olefinic compounds. *Xenobiotica* 1973; **3**:305–340.
87. Guenthner TM, Oesch F. Metabolic activation and inactivation of chemical mutagens and carcinogens. *Trends Pharmacol Sci* 1981; **2**:129–132.
88. Glatt HR, Wölfel T, Oesch F. Determination of epoxide hydrolase activity in whole cells (human lymphocytes) and activation by benzoflavones. *Biochem Biophys Res Commun* 1983; **110**:525–529.
89. Skoda RC, Demierre A, McBride OW, Gonzalez FJ, Meyer UA. Human microsomal xenobiotic epoxide hydrolase. Complementary DNA sequence, complementary DNA-directed expression in COS-1 cells, and chromosomal localization. *J Biol Chem* 1988; **263**:1549–1554.
90. Hartsfield J, Sutcliffe MJ, Everett E, Hassett C, Omiecinski CJ, Saari JA. Assignment of microsomal epoxide hydrolase (EPHX1) to human chromosome 1q42.1 by in situ hybridization. *Cytogenet Cell Genet* 1998; **83**:44–45.
91. Beetham JK, Tian TG, Hammock BD. cDNA cloning and expression of a soluble epoxide hydrolase from human liver. *Arch Biochem Biophys* 1993; **305**:197–201.
92. Larsson C, White I, Johansson C, Stark A, Meijer J. Localization of the human soluble epoxide hydrolase gene (EPHX2) to chromosomal region 8p21-p12. *Hum Genet* 1995; **95**:356–358.
93. Zhou X, Zheng Y. Cell type-specific signaling function of RhoA GTPase: lessons from mouse gene targeting. *J Biol Chem* 2013; **288**:36179–36188.
94. Xiong X, Zhao Y, Tang F, Wei D, Thomas D, Wang X, Liu Y, Zheng P, Sun Y. Ribosomal protein S27-like is a physiological regulator of p53 that suppresses genomic instability and tumorigenesis. *Elife* 2014; **3**:e02236.
95. Ko LJ, Prives C. p53: Puzzle and paradigm. *Genes Dev* 1996; **10**:1054–1072.
96. Barreyro L, Sampson AM, Bolanos L, Niederkorn M, Pujato M, Smith MA, Tomoya M, Haffey WD, Christie S, Liu X, Weirauch M, Greis K et al. Inhibition of UBE2N as a therapeutic approach in myelodysplastic syndromes (MDS) and acute myeloid leukemia (AML). *Blood* 2016; **128**:579–579.
97. Yu Y, Wang X-Y, Sun L, Wang Y-L, Wan Y-F, Li X-Q, Feng Y-M. Inhibition of KIF22 suppresses cancer cell proliferation by delaying mitotic exit through upregulating CDC25C expression. *Carcinogenesis* 2014; **35**:1416–1425.
98. Zhang C, Li A, Li H, Peng K, Wei Q, Lin M, Liu Z, Yin L, Li J. PPP1R12A copy number is associated with clinical outcomes of stage III CRC receiving oxaliplatin-based chemotherapy. *Mediators Inflamm* 2015; **2015**:417184.
99. Watt PM, Hickson ID. Structure and function of type II DNA topoisomerases. *Biochem J* 1994; **303**:681–695.
100. Lucio-Eterovic AK, Singh MM, Gardner JE, Veerappan CS, Rice JC, Carpenter PB. Role for the nuclear receptor-binding SET domain protein 1 (NSD1) methyltransferase in coordinating lysine 36 methylation at histone 3 with RNA polymerase II function. *Proc Natl Acad Sci* 2010; **107**:16952.
101. Huang N, vom Baur E, Garnier JM, Lerouge T, Vonesch JL, Lutz Y, Chambon P, Losson R. Two distinct nuclear receptor interaction domains in NSD1, a novel SET protein that exhibits characteristics of both corepressors and coactivators. *EMBO J* 1998; **17**: 3398–3412.
102. Kawaguchi R, Yu J, Honda J, Hu J, Whitelegge J, Ping P, Wiita P, Bok D, Sun H. A membrane receptor for retinol binding protein mediates cellular uptake of vitamin a. *Science* 2007; **315**:820–825.
103. Bouillet P, Sapin V, Chazaud C, Messaddeq N, Décimo D, Dollé P, Chambon P. Developmental expression pattern of Stra6, a retinoic acid-responsive gene encoding a new type of membrane protein. *Mech Dev* 1997; **63**:173–186.
104. Berry DC, Jin H, Majumdar A, Noy N. Signaling by vitamin A and retinol-binding protein regulates gene expression to inhibit insulin responses. *Proc Natl Acad Sci* 2011; **108**:4340–4345.
105. Berry DC, O'Byrne SM, Vreeland AC, Blaner WS, Noy N. Cross talk between signaling and vitamin a transport by the retinol-binding protein receptor STRA6. *Mol Cell Biol* 2012; **32**:3164–3175.
106. Berry DC, Croniger CM, Ghyselinck NB, Noy N. Transthyretin blocks retinol uptake and cell signaling by the holo-retinol-binding protein receptor STRA6. *Mol Cell Biol* 2012; **32**:3851–3859.

107. Peters J-M, Tedeschi A, Schmitz J. The cohesin complex and its roles in chromosome biology. *Genes Dev* 2008; **22**:3089–3114.
108. Rauhala HE, Teppo S, Niemelä S, Kallioniemi A. Silencing of the ARP2/3 complex disturbs pancreatic cancer cell migration. *Anticancer Res* 2013; **33**:45–52.
109. Mullins RD, Heuser JA, Pollard TD. The interaction of Arp2/3 complex with actin: Nucleation, high affinity pointed end capping, and formation of branching networks of filaments. *Proc Natl Acad Sci* 1998; **95**:6181–6186.
110. Welch MD, DePace AH, Verma S, Iwamatsu A, Mitchison TJ. The human Arp2/3 complex is composed of evolutionarily conserved subunits and is localized to cellular regions of dynamic actin filament assembly. *J Cell Biol* 1997; **138**:375–384.
111. Yoo Y, Wu X, Guan JL. A novel role of the actin-nucleating Arp2/3 complex in the regulation of RNA polymerase II-dependent transcription. *J Biol Chem* 2007; **282**:7616–7623.
112. Schrank BR, Aparicio T, Li Y, Chang W, Chait BT, Gundersen GG, Gottesman ME, Gautier J. Nuclear ARP2/3 drives DNA break clustering for homology-directed repair. *Nature* 2018; **559**:61–66.
113. Rensen WM, Roscioli E, Tedeschi A, Mangiacasale R, Ciciarello M, Di Gioia SA, Lavia P. RanBP1 downregulation sensitizes cancer cells to taxol in a caspase-3-dependent manner. *Oncogene* 2009; **28**:1748–1758.
114. Cover PO, Baanah-Jones F, John CD, Buckingham JC. Annexin 1 (lipocortin 1) mimics inhibitory effects of glucocorticoids on testosterone secretion and enhances effects of interleukin-1β. *Endocrine* 2002; **18**:33–39.
115. Tsao FHC, Chen X, Chen X, Ts'ao C-H. Annexin I in female rabbit reproductive organs: Varying levels in relation to maturity and pregnancy. *Lipids* 1995; **30**:507–511.
116. Sun M, Liu Y, Gibb W. Distribution of annexin I and II in term human fetal membranes, decidua and placenta. *Placenta* 1996; **17**:181–184.
117. Hebeda CB, Machado ID, Reif-Silva I, Moreli JB, Oliani SM, Nadkarni S, Perretti M, Bevilacqua E, Farsky SHP. Endogenous annexin A1 (AnxA1) modulates early-phase gestation and offspring sex-ratio skewing. *J Cell Physiol* 2018; **233**:6591–6603.
118. Römisch J, Schüler E, Bastian B, Bürger T, Dunkel FG, Schwinn A, Hartmann AA, Pâques EP. Annexins I to VI: quantitative determination in different human cell types and in plasma after myocardial infarction. *Blood Coagul Fibrinolysis* 1992; **3**:11–17.
119. Moravcikova E, Krepela E, Prochazka J, Rousalova I, Cermak J, Benkova K. Down-regulated expression of apoptosis-associated genes APIP and UACA in non-small cell lung carcinoma. *Int J Oncol* 2012; **40**:2111–2121.
120. Lasek AW. Effects of ethanol on brain extracellular matrix: implications for alcohol use disorder. *Alcohol Clin Exp Res* 2016; **40**:2030–2042.
121. Stephens DN, King SL, Lambert JJ, Belelli D, Duka T. GABAA receptor subtype involvement in addictive behaviour. *Genes Brain Behav* 2017; **16**:149–184.
122. Gravel RA, Kaback MM, Proia RL, Sandhoff K, Suzuki K, Suzuki K. The GM2 Gangliosidoses. In: *The Metabolicand Molecular Bases of Inherited Disease*, vol. **3**, 8th ed. New York, USA: McGraw-Hill; 2001: 3827–3876.
123. Trasler J, Saberi F, Somani IH, Adamali HI, Huang J-Q, Fortunato SR, Ritter G, Gu M, Aebersold R, Gravel RA, Hermo L. Characterization of the testis and epididymis in mouse models of human Tay Sachs and Sandhoff diseases and partial determination of accumulated gangliosides∗. *Endocrinology* 1998; **139**:3280–3288.
124. Ziff JL, Crompton M, Powell HR, Lavy JA, Aldren CP, Steel KP, Saeed SR, Dawson SJ. Mutations and altered expression of SERPINF1 in patients with familial otosclerosis. *Hum Mol Genet* 2016; **25**:2393–2403.
125. Dawson DW, Volpert OV, Gillis P, Crawford SE, Xu H, Benedict W, Bouck NP. Pigment epithelium-derived factor: a potent inhibitor of angiogenesis. *Science* 1999; **285**:245–248.
126. Homan EP, Rauch F, Grafe I, Lietman C, Doll JA, Dawson B, Bertin T, Napierala D, Morello R, Gibbs R, White L, Miki R et al. Mutations in SERPINF1 cause osteogenesis imperfecta type VI. *J Bone Miner Res* 2011; **26**:2798–2803.
127. Chuderland D, Ben-Ami I, Bar-Joseph H, Shalgi R. Role of pigment epithelium-derived factor in the reproductive system. *Reproduction* 2014; **148**:R53–R61.
128. Kuiper GG, Lemmen JG, Carlsson B, Corton JC, Safe SH, van der Saag PT, van der Burg B, Gustafsson JA. Interaction of estrogenic chemicals and phytoestrogens with estrogen receptor beta. *Endocrinology* 1998; **139**:4252–4263.
129. Sailland J, Tribollet V, Forcet C, Billon C, Barenton B, Carnesecchi J, Bachmann A, Gauthier KC, Yu S, Giguère V, Chan FL, Vanacker J-M. Estrogen-related receptor α decreases RHOA stability to induce orientated cell migration. *Proc Natl Acad Sci* 2014; **111**:15108–15113.
130. Malissein E, Meunier E, Lajoie-Mazenc I, Médale-Giamarchi C, Dalenc F, Doisneau-Sixou SF. RhoA and RhoC differentially modulate estrogen receptor α recruitment, transcriptional activities, and expression in breast cancer cells (MCF-7). *J Cancer Res Clin Oncol* 2013; **139**:2079–2088.
131. Liu X, An BH, Kim MJ, Park JH, Kang YS, Chang M. Human glutathione S-transferase P1-1 functions as an estrogen receptor α signaling modulator. *Biochem Biophys Res Commun* 2014; **452**:840–844.
132. Prenzel T, Kramer F, Chanana U, Nagarajan S, Beißbarth T, Johnsen S. Cohesin is required for expression of the estrogen receptor-alpha (ESR1) gene. *Epigenetics Chromatin* 2012; **5**:13.
133. Ang EZ-F, Nguyen HT, Sim H-L, Putti TC, Lim LHK. Annexin-1 regulates growth arrest induced by high levels of estrogen in MCF-7 breast cancer cells. *Mol Cancer Res* 2009; **7**:266–274.
134. Lowy CM, Oskarsson T. Tenascin C in metastasis: a view from the invasive front. *Cell Adh Migr* 2015; **9**:112–124.
135. Varshney MK, Inzunza J, Lupu D, Ganapathy V, Antonson P, Rüegg J, Nalvarte I, Gustafsson J-Å. Role of estrogen receptor beta in neural differentiation of mouse embryonic stem cells. *Proc Natl Acad Sci* 2017; **114**:E10428–E10437.
136. Franco-Chuaire ML, Ramírez-Clavijo S, Chuaire-Noack L. Pigment epithelium-derived factor: clinical significance in estrogen-dependent tissues and its potential in cancer therapy. *Iran J Basic Med Sci* 2015; **18**:837–855.
137. Sparano JA, Goldstein LJ, Davidson NE, Sledge GW Jr, Gray R. TOP2A RNA expression and recurrence in estrogen receptor-positive breast cancer. *Breast Cancer Res Treat* 2012; **134**:751–757.
138. Pavone ME, Reierstad S, Sun H, Milad M, Bulun SE, Cheng Y-H. Altered retinoid uptake and action contributes to cell survival in endometriosis. *J Clin Endocrinol Metab* 2010; **95**:E300–E309.